Analytica Chimica Acta 1202 (2022) 339675

Contents lists available at ScienceDirect

Analytica Chimica Acta

journal homepage: www.elsevier.com/locate/aca

Ultrasensitive electrochemical biosensor for protein detection based on target-triggering cascade enzyme-free signal amplification strategy

Pinghua Ling *, Linyu Wang , Shan Cheng , Xianping Gao , Xinyu Sun , Feng Gao **

Laboratory of Functionalized Molecular Solids, Ministry of Education, Anhui Key Laboratory of Chemo/Biosensing, College of Chemistry and Materials Science, Anhui Normal University, Wuhu, 241002, PR China

HIGHLIGHTS

- Electrochemical detection of thrombin using target-triggering cascade enzyme-free signal amplification strategy was proposed.
- The method was PCR-free, enzyme-free, low cost, and without the need for any additional separation steps.
- The sensor for thrombin showed good performance.

GRAPHICAL ABSTRACT

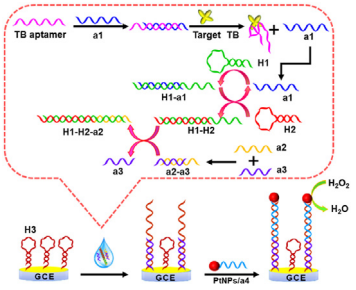

ARTICLE INFO

Article history:
Received 2 February 2022
Received in revised form
24 February 2022
Accepted 2 March 2022
Available online 4 March 2022

Keywords:
Electrochemical biosensor
Thrombin
Enzyme-free
Signal amplification

ABSTRACT

Herein, a cost-effective, simple and sensitive electrochemical sensing platform was established based on aptamer - target recognition and target-triggering signal amplification strategy for protein detection. Due to the high affinity between the aptamer and target, the assistant DNA1 (a1) could release from a1-aptamer duplex and trigger the following DNA circuits. The strand displacement and branch migration reaction brought assistant DNA3 (a3) released. Eventually, a large number of duplex structures of a3−Hairpin DNA3 were formed on the surface of electrode. Consequently, the capture DNA on the surface of platinum nanoparticles could hybridize with the unfolded DNA fragment of Hairpin DNA3 on the sensor surface, resulting in the electrochemical signal readout of H_2O_2 reduction. Using thrombin as a model target, under the optimal conditions, this method exhibited a linear detection range from 0.5 pM to 300 nM with a detection limit of 0.17 pM. The proposed detection strategy was enzyme-free and exhibited good selectivity and sensitivity for a variety of protein targets detection by using corresponding DNA-based affinity probes, which makes it possible to apply the sensor for sensitivity detection of analytes in bioassays.

1. Introduction

Thrombin (TB) which is a kind of allosteric serine protease, has an important role in human life and participates in several bioregulatory processes, such as blood coagulation cascade [1,2], inflammation reactions [3], blood circulation [4], anticlotting therapeutics [5,6], and so on [7,8]. Besides, evidences have been reported that thrombin was also used as a biomarker for the

* Corresponding author.
** Corresponding author.
E-mail addresses: phling@ahnu.edu.cn (P. Ling), fgao@mail.ahnu.edu.cn (F. Gao).

https://doi.org/10.1016/j.aca.2022.339675
0003-2670/

diagnosis of certain diseases [9] and its abnormality expression is closely related to various human diseases such as tumor growth [10] metastases [11], angiogenesis [12], and myocardial infarction [13]. Thus, the sensitive, quantitative and selective detection of thrombin activity is imperative to the evaluation of ability of blood and the diagnosis of coagulation disorder-related diseases.

Aptamers which are single stranded DNA or RNA with 25–60 nucleotides in length [14,15], are isolated from random nucleic acid libraries and have been widely used in disease diagnosis and bioassays since their first report in 1990 [14,16]. Aptamers exhibited numerous advantages such as convenient synthesis, stable structure, easy separation and modification, highly binding affinity and specificity recognize various targets including proteins, peptides, small molecules, even cells as well [17–20], which makes aptamers superior to antibody probes. Due to the unique merit, aptamers have seen used as recognition element for cancer therapy and to fabricate biosensor for pathological diagnosis, pharmaceutical analysis and environmental monitoring [21–24].

Hitherto, numerous methods based on aptamer pairs have been developed to detect thrombin, such as chemiluminescence [23,25], colorimetry [26,27], fluorescence [28–30], electrochemistry [31–36], and surface-enhanced Raman scattering (SERS)-based [37,38] etc. These methods have high specificity and sensitivity simple operation, wide linear range and could meet the requirements of the analysis. Among these methods, electrochemical sensing with simple equipment and operation, and lower consumption has attracted immense interest in recent years. Currently [34], designed a sensitive electrochemical aptasensor for thrombin detection using nicking endonuclease for signal amplification and quite complex interfacial and reactant/catalytic labels designs such as Co-MOF decorated with PtPd nanoparticles [39]. reported an amplified electrochemical biosensor for the detection of thrombin activity by reversible addition–fragmentation chain ransfer (RAFT) polymerization. However, they suffer from somewhat drawbacks, such as expensive and complex modifications, which make them less suitable for immediate clinical applications. Therefore, it is still needed to design a more economical, sensitive, good stability and simple strategy for thrombin detection.

Herein, we developed a simple yet sensitive biosensor based on target-triggering cascade enzyme-free signal amplification strategy for the detection of thrombin (Fig. 1). First, hairpin DNA3 (H3) was bonded to the gold nanoparticle (AuNPs)-modified electrode surface via the Au–S bond. In the presence of thrombin, assistant DNA1 (a1) was released due to the recognition reaction between the TB aptamer and thrombin [14,15,17,34,40,41]. Then, the released a1 could hybridize with hairpin DNA1 (H1). Next, in the presence of hairpin DNA2 (H2), H1 could hybridize with H2 to form H2–H1 duplex, leading to a1 dissociated from the H1–a1 duplex. The released a1 will be reused to initiate the repeated rounds of strand displacement, which produced numerous H1–H2 duplexes. Next, the generated H1–H2 duplex continued to hybridize with assistant DNA2 (a2) – assistant DNA3 (a3) duplex via branch migration reaction to obtain H1–H2-a2 complex and released a3. Meanwhile, the output a3 could hybridize with H3 on the surface of electrode to unfold the hairpin loop of H3. After many cyclic processes, numerous unfolded DNA fragments of H3 could be generated and hybridized with capture DNA (a4) on the surface of platinum nanoparticles (PtNPs), resulting in that a great deal of a4–conjugated nanomaterials (PtNPs/a4) could be introduced on the electrode surface, leading to an enhanced current of electrocatalytic reduction toward H_2O_2 for readout. However, H1 and H2 cannot spontaneously hybridize with each other in the absence of a1, due to the effective block created by intramolecular hairpin structures. Therefore, with such design, the developed method possessed high sensitivity for thrombin detection with a detection limit down to 0.17 pM. Furthermore, the biosensor exhibited good stability, reproducibility, and specificity, due to aptamer recognition and enzyme-free DNA recycle signal amplification process, implying a promising potential for sensitive protein biomarkers detection.

2. Experimental

2.1. Materials and reagents

Thrombin (TB), chloroplatinic acid (H_2PtCl_6), sodium borohydride ($NaBH_4$), L-cysteine (L-Cys), 6-mercapto-1-hexanol (MCH) and hemoglobin (Hem) were obtained from Sigma-Aldrich Chemical Co (St. Louis, MO, U.S.A.). Gold chloride ($HAuCl_4$) and sodium nitrate ($NaNO_3$) were purchased form Sinopharm (China). Bovine serum albumin (BSA), immunoglobulin G (IgG), lactic acid (LA), horseradish peroxidase (HRP), human serum albumins (HSA) and all DNA sequences were purchased from Sangon Biotech Co., Ltd. (Shanghai, China). All DNA sequences were designed according to the base matching rules and analyzed with OligoAnalyzer, an online nucleic acid analysis software. The sequences of the oligonucleotides were used in this study as follows:

TB aptamer: 5'-GGT TGG TGT GGT TGG AGA AGA AGG TGT TTA AGTA-3
Assistant DNA1 (a1): 5'-CGA CAT CTA ACC TAG CTC ACT GAC CCA ACC ACA CCA ACC-3
Assistant DNA2 (a2): 5'-GCT GAG ATT TTC CAC ACT GAC TGC TAG GTT - 3
Assistant DNA3 (a3): 5'-GAA GTC AGT GTG GAA AAT CTC TAG C-3
Capture DNA4 (a4): 5'–SH–(CH2)6-TTT TCC ACA CTG ACT AAA ACC CAA AAC C-3
Hairpin DNA 1 (H1): 5'-GTC AGT GAG CTA GGT TAG ATG TCG CCA TGT GTA GAC GAC ATC TAA CCT AGC AGT CAG TGT GGA AAA TCT CTA GC-3
Hairpin DNA 2 (H2): 5'-AGA TGT CGT CTA CAC ATG GCG ACA TCT AAC CTA GCC CAT GTG TAG A-3
Hairpin DNA 3 (H3): 5'–SH–(CH2)6-GCT AGA GAT TTT CCA CAC TGA CTT CTC TAG CGG GTT TTG GGT TTT AGT CAG TGT GGA AAA-3

In this work, 20 mM Tris-HCl buffer (pH 7.4) containing 140 mM NaCl, 5 mM KCl and 1.0 mM $MgCl_2$ was used as oligonucleotide stock solutions. Thrombin digestion buffer was prepared with 10 mM Na_2HPO_4, 10 mM NaH_2PO_4, and 2.0 mM $MgCl_2$. 0.1 M PBS (pH 7.4) was used as electrolyte solution. Prior to use, all oligonucleotides were heated to 90 °C for 10 min and then cooled down to room temperature. Serum samples were obtained from Second People's Hospital of Wuhu, China and properly diluted by pH 7.4 PBS buffer when the levels of thrombin were over the calibration range. All reagents were analytical grade. Ultrapure water (≥18.25 MΩ, Milli-Q, Millipore) was employed to prepare buffer solutions.

2.2. Apparatus

The transmission electron microscopy (TEM) images were operated on a JEOL JEM-2010 microscope. UV–vis absorption spectra were performed on a Hitachi U-3900 UV/vis spectrometer (Hitachi, Japan). Powder X-ray diffraction (XRD) patterns were carried on X-ray powder diffractometer operating at 40 kV and 40 mA (CuKα radiation, λ = 1.5418 Å). Polyacrylamide gel electrophoresis (10%) (PAGE) was obtained on the electrophoresis apparatus (DYCP-31DN, Beijing Liuyi Biotechnology Co., Ltd) and imaged on FUSION FX7 EDGE (VILBER LOURMAT, France). Cyclic

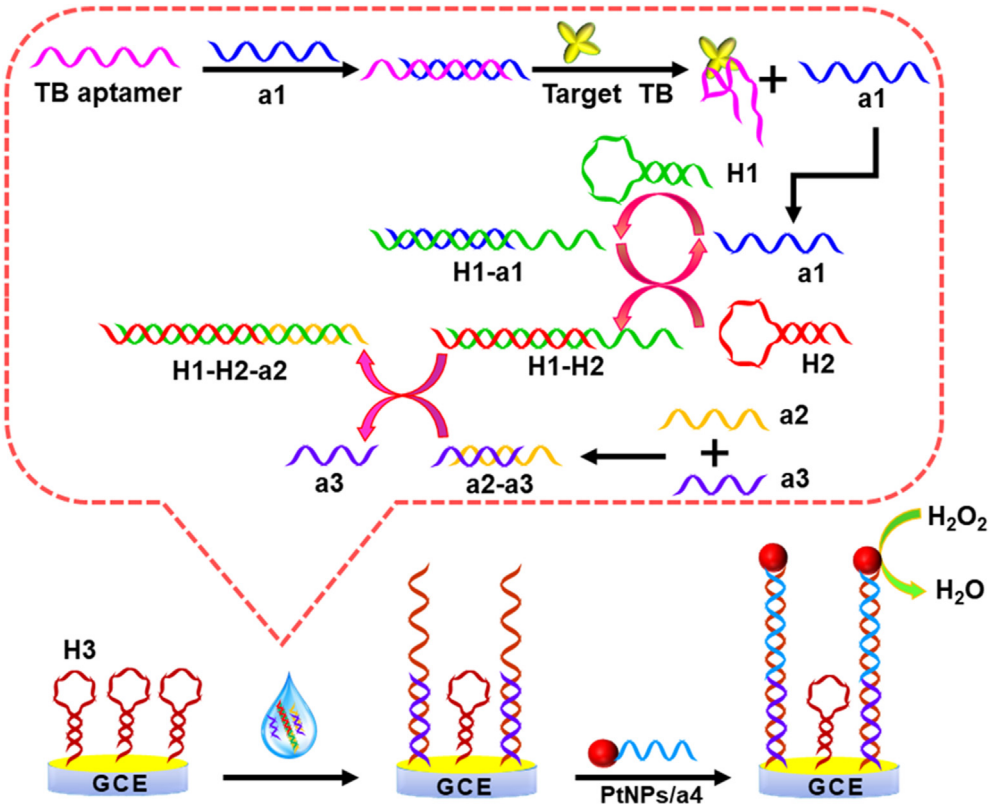

Fig. 1. Schematic illustration of electrochemical detection strategy for thrombin activity via target-triggering cascade enzyme-free signal amplification strategy.

voltammetry (CV) and differential pulse voltammograms (DPV) were performed using a CHI 760E electrochemical workstation (Shanghai CH Instruments, China) at room temperature. The three-electrode system are composed of a glassy carbon electrode (GCE) working electrode, an Ag/AgCl reference electrode and a counter electrode of platinum wire.

2.3. Preparation of PtNPs

The PtNPs were synthesized by adding 5.0 mL fresh ice-cold $NaBH_4$ solution (0.01 M) to 4.0 mL H_2PtCl_6 aqueous solution (2.0 mM). After stirring vigorously for 20 min, the product was centrifuged and washed with water for several times.

2.4. Synthesis of PtNPs/a4

Typically, in order to break the disulfide bond, the thiol terminated a4 was incubated with TCEP (1.0 mM) for 1 h at room temperature. Then, a volume of 300 μL of TCEP-pretreated a4 (100 μM) were added into 1.0 mL of PtNPs, and then stirred overnight under 4 °C. Finally, the obtained product was centrifuged and washed with 0.1 M PBS buffer (pH 7.4), and then resuspended in 1.0 mL of PBS.

2.5. Fabrication of biosensor and electrochemical detection

Initially, 20 μL TB aptamer (2.0 μM) and 20 μL a1 (2.0 μM) were injected in tube for 2 h at 37 °C. Subsequently, different concentrations of thrombin were injected in the abovementioned tube for 3 h at 37 °C, then a different amount of released a1 was obtained. Meanwhile, 20 μL a2 (2.0 μM) and 20 μL a3 (2.0 μM) were incubated at 37 °C for 2 h to form a2-a3 duplex.

For the recycle process, the released a1 solution (40 μL), H1 solution (2.0 μM, 20 μL), and H2 solution (2.0 μM, 20 μL) were mixed and incubated at 37 °C for 45 min. Then, 20 μL a2-a3 duplex was added and incubated at 37 °C for 2 h. The resulting mixture was ready to use in the next electrochemical experiment or stored at 4 °C.

Prior to experiment, the GCE was carefully polished sequentially with 1.0, 0.3 and 0.05 μm alumina powder, followed washing by sonication in deionized water and ethanol for 5 min and dried in nitrogen. After the GCE cleaned, it was dipped into 0.1 M $NaNO_3$ containing $HAuCl_4$ solution (1.0 mg/mL) and electrodeposited at −0.2 V for 600 s to obtain a layer of gold nanoparticles (AuNPs).

Then, the AuNPs modified GCE was incubated with 15 μL of TCEP-pretreated H3 (2.0 μM) for about 16 h at room temperature. Subsequently, 15 μL of MCH (1.0 mM) was dropped to block the nonspecific combining sites, followed 15 μL the reaction mixture (TB aptamer + a1 + H1 + H2 + a2-a3) was dropped onto the MCH/H3/Au/GCE electrode and incubated for 3 h at 37 °C to unfold the H3. After washing, the electrode was incubated with 15 μL of the PtNPs/a4 for 2 h at 37 °C. Eventually, the biosensor was washed and tested in 0.1 M PBS containing 10 mM H_2O_2.

2.6. Gel electrophoresis

The gel electrophoresis was performed by injecting the mixture including 7.0 μL of samples, 1.5 μL loading buffer and 1.5 μL GelRed into a 10% polyacrylamide hydrogel in tris-borate-EDTA (TBE) buffer. Electrophoresis was carried out at 100 V in TBE buffer for 1 h, and observed under UV irradiation.

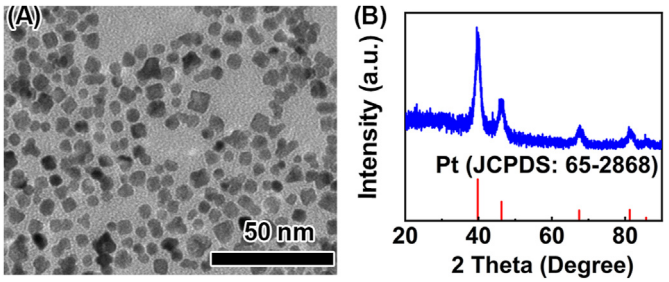

Fig. 2. (A) TEM images and (B) XRD of PtNPs.

3. Results and discussion

3.1. Characterization of PtNPs

Fig. 2A depicts the transmission electron microscopy (TEM) image of PtNPs. The diameter of obtained PtNPs was ca. 10 nm and dispersed uniformly. The XRD displayed that the charactered peaks of PtNPs at 40-80° (JCPDS: 65−2868) were observed, revealing that the PtNPs were successfully formed (Fig. 2B).

3.2. Characterization of feasibility of the electrochemical sensor

Cyclic voltammetry (CV) measurements were employed to characterize the preparation and electrochemical properties of the biosensor in 0.1 M KCl containing 5 mM $K_3Fe(CN)_6$ and $K_4Fe(CN)_6$ (Fig. 3). The bare electrode showed a well-defined redox wave due to the reversible redox reaction of ferricyanide ions on the surface of the bare GCE electrode (curve a). When the AuNPs was modified on the electrode, the redox peak current increased owing to the better conductive ability of AuNPs (curve b). After H3 was captured on the AuNPs/GCE (curve c), the current decreased, which because H3 can increase severely the steric hindrance and obstruct the electron transfer of the redox probe, indicating the successful modification of H3. Next, when the electrode was incubated with the reaction mixture containing TB aptamer, a1, H1, H2, a2 and output a3, a further decrease in the redox peak current was observed (curve d), which because the output a3 could bind to H3, resulting in retarding the electron transfer. Because the better

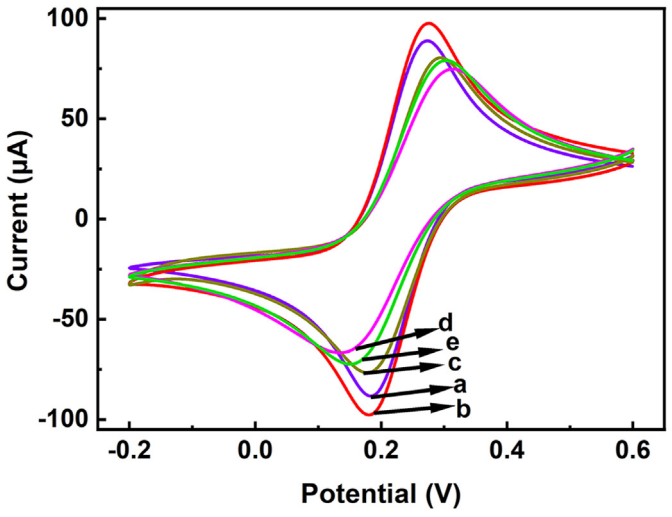

Fig. 3. CVs of the different modified electrode at 50 mV/s in 5 mM $[Fe(CN)_6]^{3-/4-}$ solution: bare GCE (a), AuNPs/GCE (b), H3/AuNPs/GCE (c), (d) a3-H3/AuNPs/GCE, (e) PtNPs/a4-a3-H3/AuNPs/GCE.

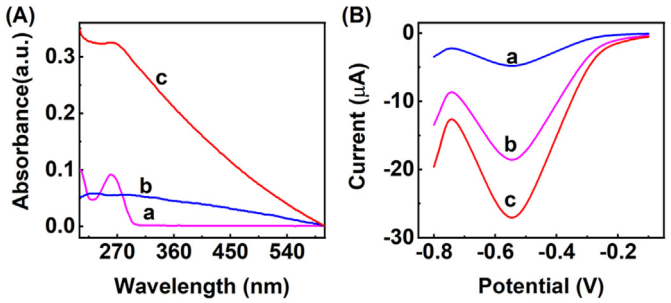

Fig. 4. (A) UV−vis absorption spectra of DNA (a), PtNPs (b) and PtNPs/a4 (c). (B) DPV response of H3 modified GCE incubated with different concentrations of thrombin, 0 pM (a), 100 pM (b) and 50 nM (c).

conductivity of PtNPs, the current increased after PtNPs/a4 was dropped on the electrode (curve e).

The enzyme-free DNA circuitry is a great important factor for signal amplification. In order to confirm the formation of PtNPs/a4, UV−vis absorption spectrometry was first employed and shown in Fig. 4A. Compared with pure PtNPs (curve b), a new absorption peak at 260 nm was observed (curve c), which is the character peak of DNA (curve a), illustrating that a4 was modified on the surface of PtNPs. Next, the feasibility of the sensor was verified by the differential pulse voltammograms (DPV) (Fig. 4B). It can be seen that the sensor showed a weak peak current at around −0.55 V in the absence of thrombin (curve a), which may be due to the nonspecific interaction between PtNPs/a4 and the AuNPs/GCE. In the presence of thrombin (100 pM), the current response increased (curve b), which implied that the thrombin could recognize TB aptamer and a1 released, then a1 could trigger the DNA recycle to amplify the current signal. Upon the addition of 50 nM thrombin, the current further increased (curve c), which should be contributed to more released a1 for DNA recycle. Thus, more a3 could be released and hybridized with H3, leading to more PtNPs/a4 were bonded to the surface of GCE to obtain a significantly amplified current signal. These results suggested the method could realize the sensitive detection of thrombin.

In addition, the feasibility of the strategy was confirmed by Gel electrophoresis (Fig. 5). Line a, b, c, d, e, f, g, and h display TB aptamer, a1, a2, a3, H1, H2, a4, and H3 bands, respectively. When TB aptamer incubated with a1, there was a new low migration rate on the gel, suggesting TB aptamer was hybridized with a1 to form TB aptamer-a1 double helix (line i), Similarly, the a1-H1 double helix formed (line j). Line k displays the bands of H1 and H2, which demonstrates that H1 and H2 could coexist stably due to being

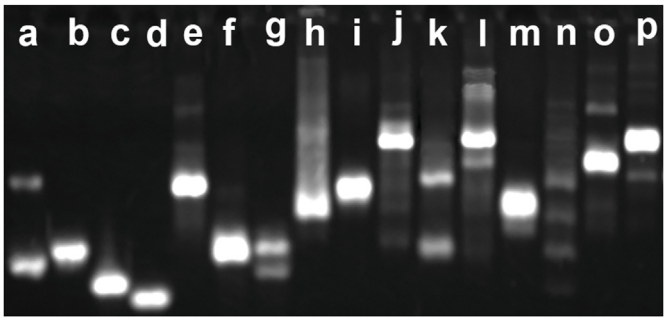

Fig. 5. PAGE electrophoresis image of different samples in the amplification assay: lane a, TB aptamer; lane b, a1; lane c, a2; lane d, a3; lane e, H1; line f, H2, line g, a4; line h, a3; line i, TB aptamer + a1; line j, a1 + H1, line k, H1 + H2; line l, a1 + H1 + H2, and line m, a2+ a3, line n, H1 + H2 + a2-a3, line o, H3 + a3, and line p, H3 + a3 + a4.

kinetically hindered. While in the presence of a1, a new band of H1−H2 duplex was observed, and the H1, H2 bands significantly reduced in line l. Line m shows the a2-a3 double helix. The bands H1, H2 and a2-a3 double helix were observed in line n, which showed that a3 could not release from a2-a3 double helix due to the hairpin structure of H1 and H2 could not be unfolded by a3. Line o showed the a3-H3 duplex formed. In the present of a4, a new band was observed (line p), which has lower migration than line o, demonstrating a3-H3-a4 duplex formed. Therefore, the designed method was feasible.

3.3. Optimization of detection conditions

In order to maximize the electrochemical signal, some experiment conditions such as incubation time for thrombin recognition, amplification time, and the hybridization time of the reaction mixture (TB aptamer, a1, H1, H2, a2 and output a3) with H3 were systematically optimized. First, the incubation time for the reaction between thrombin and TB aptamer is an important parameter that impacts the analysis performance of the sensor. As displayed in Fig. 6A, the electrochemical signal change first increased quickly and remained steady at approximately 3 h with the increasing of the incubation time, which indicates that the binding of the TB aptamer and thrombin was saturated. So, the optimal incubation time was selected 3 h.

The reaction time of recycle process is another major factor influencing the amplification signal; too short an amplification time cannot produce sufficient a3. Depicted in Fig. 6B is the effect of amplification times to the current signal in the range from 0.5 to 4 h. It can be seen that with the increasing of amplification times, the current signal increased and then reached a balance beyond 3 h. Therefore, 3 h was long enough for the signal amplification process, and was chosen as the optimal reaction time of recycle.

Additionally, the hybridization time between the reaction mixture (TB aptamer, a1, H1, H2, a2 and output a3) and H3 mainly influences the current signal. The incubation time is too short, little H3 was unfolded, leading to little PtNPs/a4 captured on the surface of the electrode. The result in Fig. 6C showed the current signal reached the maximum value with the incubation time for 2 h. After 2 h, the peak current has no obvious change. Then, the optimal incubation time for the reaction mixture hybridization with a3 was selected 2 h.

3.4. Detection of thrombin

With the optimal experimental parameters, various concentration of thrombin was measured with DPV to evaluate the sensitivity of the present electrochemical sensor. The DPV current response regularly enhanced with increasing the concentration of thrombin

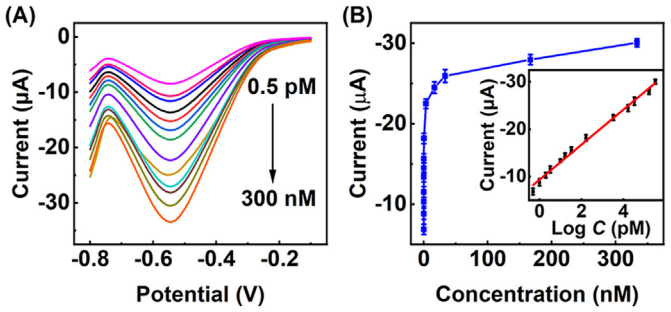

Fig. 7. (A) DPV signals of a range of thrombin: 0.5 pM, 1.0 pM, 2.0 pM, 3.0 pM, 10 pM, 15 pM, 30 pM, 160 pM, 3.0 nM, 15 nM, 30 nM, 160 nM and 300 nM. (B) Dependence of DPV peak currents on thrombin concentrations. Inset: calibration curve of current intensity vs logarithmic value of thrombin concentration. The potential was at −0.55 V (vs Ag/AgCl).

(Fig. 7A). Furthermore, the peak current showed a linear range with logarithm of thrombin concentration from 0.5 pM to 300 nM with a corresponding correlation coefficient (R^2) of 0.994 (Fig. 7B). The detection limit value was estimated to be 0.17 pM at signal-to-noise ratio of 3, which was lower than that of previous reported by DPV (5.6 pM [42] and 3 pM [35]). And the comparison of this method with other methods were also shown in Table S1. The better detection of limit of this sensor may be attributed to the high amplification efficiency and good conductivity and catalytic ability of PtNPs.

3.5. Selectivity, reproducibility, and stability of sensor

In order to examine the selectivity of the present method for thrombin detection, some interferences including L-cysteine (L-Cys), hemoglobin (Hem), albumin (BSA), immunoglobulin G (IgG), lactic acid (LA), Horseradish peroxidase (HRP), Human serum slbumins (HSA) and hemoglobin (Hb) were tested under the same experiment conditions (Fig. S1). It can be seen that the peak current with the presence of L-Cys, Hem, BSA, lgG, LA, HRP, HAS and Hb at the concentration of 150 nM is lower than that of 3 nM thrombin, indicating the sensor had good selectivity.

To investigate the reproducibility of the sensor, nine electrodes were prepared and employed to detect 3 nM thrombin. The obtained relative standard deviation (RSD) is 4.10%. In addition, the sensor was used to test 3 nM thrombin for nine times with RSD of 4.37%. The results implied the sensor had good reproducibility and repeatability. The sensor was stored at 4 °C before use for two weeks and tested each day. The electrochemical signal retained 86.52% of its initial electrochemical signal, suggesting the present sensor had satisfactory stability (Fig. S2).

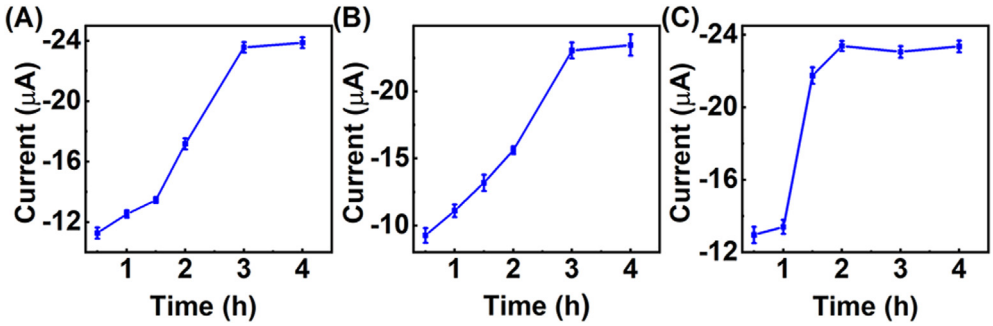

Fig. 6. Effects of (A) incubation time of thrombin and TB aptamer, (B) amplification time, (C) the hybridization time between the reaction mixture (TB aptamer, a1, H1, H2, a2 and output a3) and H3.

3.6. Application in human serum sample

The sensor was tested in serum samples (obtained from Second People's Hospital of Wuhu, China) to evaluate its practical application (Fig. S3). When the sensor was detected in human serum, high current response was obtained, and the decreased current could be negligible, demonstrating the biosensor could be applied for thrombin detection in real sample.

4. Conclusions

In the present study, a simple and sensitive electrochemical sensing platform has been developed for protein detection by employing a designed enzyme-free DNA circuits for signal amplification. By means of the aptamer - target recognition, strand displacement and branch migration reaction, the target-induced DNA circuits to successively open surface-tethered H3 and capture PtNPs/a4 on the electrode surface, generating an amplified electrochemical signal. The one-to-all amplification strategy endows the assay with high detection sensitivity and low detection limit. In addition, the method uses the DNA based assembly for signal amplification, which makes it simple and cost-efficient for protein detection, indicating potential application in bioanalysis. However, this method is time-consumption. The prospective future is focused on exploring the method with fast and accurate to detect the analyte in vivo.

CRediT authorship contribution statement

Pinghua Ling: Funding acquisition, Writing – review & editing, Planning the projects and Designing the experiment, Supervision, and Coordinated all investigators for this project. **Linyu Wang:** Data curation, Performing the experiments. **Shan Cheng:** Data curation, Performing the experiments. **Xianping Gao:** Investigation, and, Validation. **Xinyu Sun:** Investigation, and, Validation. **Feng Gao:** Writing – review & editing, Funding acquisition, Planning the projects and Designing the experiment, Supervision, and Coordinated all investigators for this project, All authors discussed the results and commented on the manuscript.

Declaration of competing interest

The authors declare that they have no known competing financial interests or personal relationships that could have appeared to influence the work reported in this paper.

Acknowledgements

We acknowledge the financial support of the National Natural Science Foundation of China (22074002, 21705004, 21874001).

Appendix A. Supplementary data

Supplementary data to this article can be found online at https://doi.org/10.1016/j.aca.2022.339675.

References

[1] E.M. Conway, J. Thromb. Haemostasis 17 (2019) 1785–1789.
[2] S.M. Prior, K.G. Mann, K. Freeman, S. Butenas, Anal. Biochem. 551 (2018) 19–25.
[3] S.R. Coughlin, Nature 407 (2000) 258–264.
[4] C. Negrier, M. Shima, M. Hoffman, Blood Rev. 38 (2019) 100582.
[5] J.J. Li, X.Q. Zhong, H.Q. Zhang, X.C. Le, J.J. Zhu, Anal. Chem. 84 (2012) 5170–5174.
[6] W.J. Xu, S.Y. Xue, H.Y. Yi, P. Jing, Y.Q. Chai, R. Yuan, Chem. Commun. 51 (2015) 1472–1474.
[7] S.P. Grover, N. Mackman, Arterioscler. Thromb. Vasc. Biol. 38 (2018) 709–725.
[8] L.K. Jennings, Thromb. Haemostasis 102 (2009) 248–257.
[9] I. Pabinger, C. Ay, Arterioscler. Thromb. Vasc. Biol. 29 (2009) 332–336.
[10] J. Zain, Y.Q. Huang, X.S. Feng, M.L. Nierodzik, J.J. Li, S. Karpatkin, Blood 95 (2000) 3133–3138.
[11] N.A. Hernández-Rodrıguez, E. Correa, A. Contreras-Paredes, L. Green, Lung Cancer 26 (1999) 157–167.
[12] H. Inuyama, T. Saito, J. Takagi, Y. Saito, J. Cell. Physiol. 173 (1997) 406–414.
[13] M.L. Nierodzik, S. Karpatkin, Cancer Cell 10 (2006) 355–362.
[14] A.D. Ellington, J.W. Szostak, Nature 346 (1990) 818–822.
[15] Y.L. Zhang, Y. Huang, J.H. Jiang, G.L. Shen, R.Q. Yu, J. Am. Chem. Soc. 129 (2007) 15448–15449.
[16] C. Tuerk, L. Gold, Science 249 (1990) 505–510.
[17] S. Centi, S. Tombelli, M. Minunni, M. Mascini, Anal. Chem. 79 (2007) 1466–1473.
[18] M. Roushani, F. Shahdost-Fard, Mater. Sci. Eng. C Mater. Biol. Appl. 68 (2016) 128–135.
[19] F. Shahdost-Fard, M. Roushani, Biosens. Bioelectron. 87 (2017) 724–731.
[20] F. Shahdost-fard, A. Salimi, S. Khezrian, Biosens. Bioelectron. 53 (2014) 355–362.
[21] X.Y. Cao, J.F. Xia, H.Z. Liu, F.F. Zhang, Z.H. Wang, L. Lu, Sens. Actuators, B 239 (2017) 166–171.
[22] M. Jarczewska, J. Rebis, L. Gorski, E. Malinowska, Talanta 189 (2018) 45–54.
[23] Y.L. Sun, X.D. Zhu, H. Liu, Y.X. Dai, R. Han, D.D. Gao, C.N. Luo, X.Y. Wang, Q. Wei, ACS Appl. Mater. Interfaces 12 (2020) 5569–5577.
[24] Z.G. Yu, A.L. Sutlief, R.Y. Lai, Sens. Actuators, B 258 (2018) 722–729.
[25] Y.N. Lin, J.B. Li, Y.H. Wang, Y.L. Sun, C.F. Ding, W.Y. Sun, C.N. Luo, Spectrochim. Acta 192 (2018) 153–158.
[26] Z.B. Chen, L.L. Tan, L.Y. Hu, Y.M. Zhang, S.X. Wang, F.Y. Lv, ACS Appl. Mater. Interfaces 8 (2016) 102–108.
[27] J.H. Park, Y.S. Cho, S. Kang, E.J. Lee, G.H. Lee, S.S. Hah, Anal. Biochem. 462 (2014) 10–12.
[28] J. Li, W.J. Zhou, R. Yuan, Y. Xiang, Anal. Chim. Acta 1038 (2018) 126–131.
[29] S. Umrao, V. Jain, Anusha, B. Chakraborty, R. Roy, Sens. Actuators, B 267 (2018) 294–301.
[30] W. Yun, L. You, F.K. Li, H. Wu, L. Chen, L.Z. Yang, Spectrochim. Acta 207 (2019) 39–45.
[31] S. Chen, P. Liu, K.W. Su, X. Li, Z. Qin, W. Xu, J. Chen, C.R. Li, J.F. Qiu, Biosens. Bioelectron. 99 (2018) 338–345.
[32] Y. Fan, F.D. Liao, W.T. Wu, N. Hong, L. Cheng, Y.Q. Zhong, H.F. Cui, G.Q. Ma, G.B. Wei, J. Xiong, H. Fan, Sens. Actuators, B 318 (2020), 128045.
[33] K. Malecka, E.E. Ferapontova, ACS Appl. Mater. Interfaces 13 (2021) 37979–37988.
[34] X. Yang, J.J. Lv, Z.H. Yang, R. Yuan, Y.Q. Chai, Anal. Chem. 89 (2017) 11636–11640.
[35] L.L. Zhang, X.Y. Zhang, P.J. Feng, Q. Han, W. Liu, Y. Lu, C.X. Song, F.Y. Li, Anal. Chem. 92 (2020) 7419–7424.
[36] Y.X. Zhang, J.F. Xia, F.F. Zhang, Z.H. Wang, Q.Y. Liu, Sens. Actuators, B 267 (2018) 412–418.
[37] Z.T. Wu, Y.F. Liu, Y.Z. Liu, H.M. Xiao, A.G. Shen, X.D. Zhou, J.M. Hu, Biosens. Bioelectron. 65 (2015) 375–381.
[38] Z.T. Wu, Y.F. Liu, X.Z. Zhou, A.G. Shen, J.M. Hu, Biosens. Bioelectron. 44 (2013) 10–15.
[39] Q. Hu, Y. Bao, S.Y. Gan, Y.W. Zhang, D.X. Han, L. Niu, Anal. Chem. 92 (2020) 3470–3476.
[40] L.C. Bock, L.C. Griffin, J.A. Latham, E.H. Vermaas, J.J. Toole, Nature 355 (1992) 564–566.
[41] D.M. Tasset, M.F. Kubik, W. Steiner, J. Mol. Biol. 272 (1997) 688–698.
[42] J.M. Yang, B.T. Dou, R. Yuan, Y. Xiang, Anal. Chem. 88 (2016) 8218–8223.